Air Shower Muons and the Atmospheric Neutrino Puzzle

S. Coutu[1], S.W. Barwick[2], J.J. Beatty[1], A. Bhattacharyya[3], C.R. Bower[3], C. Chaput[4], G.A. deNolfo[5], M.A. DuVernois[1], A. Labrador[6], S. McKee[4], D. Müller[6], J.A. Musser[3], S.L. Nutter[7], E. Schneider[2], S.P. Swordy[6], G. Tarlé[4], A.D. Tomasch[4], and E. Torbet[6]

[1]*Department of Physics, The Pennsylvania State University, University Park, PA 16802, USA*
[2]*Department of Physics, University of California, Irvine, Irvine, CA 92717, USA*
[3]*Department of Physics, Indiana University, Bloomington, IN 47405, USA*
[4]*Department of Physics, University of Michigan, Ann Arbor, MI 48109-1120, USA*
[5]*Department of Physics, Washington University, St. Louis, MO 63130, USA*
[6]*Enrico Fermi Institute and Department of Physics, University of Chicago, Chicago, IL 60637, USA*
[7]*Department of Physical Sciences, Eastern New Mexico University, Portales, NM 88130, USA*

Abstract

The study of atmospheric neutrinos and their interpretation in terms of oscillations require a detailed theoretical understanding of atmospheric neutrino production. Muon production in the atmosphere is closely coupled with neutrino production, so that measured muon fluxes can be used to calibrate neutrino production calculations. The High-Energy Antimatter Telescope (HEAT) balloon-borne magnet spectrometer was designed for the study of high-energy electrons and positrons in the cosmic-ray flux. It uses an array of redundant particle detectors suitable for the identification of other particle species as well, including muons. During atmospheric ascent of the balloon, air-shower particles have been detected in situ, and in particular the energy spectra of air-shower muons have been measured from 0.2 to 50 GeV, as a function of atmospheric depth. This measurement is described, and its implications on our understanding of atmospheric neutrino production are discussed.

1 Introduction

Measurements of the flux of atmospheric neutrinos by large underground detectors have consistently disagreed with theoretical expectations, a fact that has been interpreted in terms of possible neutrino oscillations (Fukuda et al. 1999). Specifically, values of the "ratio of ratios" $(\nu_\mu/\nu_e)_{experimental}/(\nu_\mu/\nu_e)_{theoretical}$ have been around 0.60 (Aglietta et al. 1989, Berger et al. 1989, Becker-Szendy et al. 1992, Fukuda et al. 1994, Goodman et al. 1995), with a discrepancy between experiment and theory presently at the $\sim 4\sigma$ level. One of the largest uncertainties in the theoretical predictions (Barr et al. 1989, Lee & Koh 1990, Honda et al. 1990, Kawasaki & Mizuta 1991, Agrawal et al. 1996) is a precise knowledge of the absolute flux of neutrinos produced in air showers, although the study of "ratios of ratios" alleviates this problem somewhat. Neutrino production in the atmosphere is strongly coupled to muon production, as both types of particles are produced together in pion and kaon decays, and as some of the muons decay to produce further neutrinos. Monte Carlo simulations of neutrino production naturally predict the spectrum of other air-shower secondaries, such as muons, as a function of atmospheric depth. The latter can be measured with a balloon-borne detector during atmospheric ascent, which provides a cross-check of the normalization of the expected atmospheric neutrino spectrum. Moreover, if such a detector includes a magnet spectrometer, separate measurements of the μ^- and μ^+ fluxes can be made. This can be done relatively easily for negative muons, as negatively charged particles other than electrons are rare in air showers (and electrons are easily rejected), while non-interacting protons generate a large background for positive muons above 1 GeV. Measurements have been performed by a number of experiments, including the MASS (Bellotti et al. 1996), HEAT (Tarlé et al. 1997), CAPRICE (Barbiellini et al. 1997), and IMAX (Krizmanic et al.) instruments and older, less sensitive balloon payloads.

With the High Energy Antimatter Telescope instrument, we have conducted measurements of air-shower muons twice during atmospheric ascent. Relative abundances of μ^+ and μ^- at momenta between 0.3 and 0.9 GeV/c for the first and second flights were reported elsewhere (Schneider et al. 1995, Tarlé et al. 1997).

Here we present measurements of the differential energy spectra of μ^- at momenta between 0.3 and 50 GeV/c, at atmospheric depths between 3 and 960 g/cm^2, made during the second flight. We compare the results with other measurements and with preliminary calculations performed with a modified version of the TARGET Monte Carlo algorithm (Agrawal et al. 1996), widely used in predicting atmospheric neutrino rates.

2 Muon Identification and Backgrounds

The instrument is described in detail elsewhere (Barwick et al. 1997). It combines a superconducting magnet spectrometer (using a drift-tube tracking hodoscope), a time-of-flight (TOF) system, a transition-radiation detector (TRD) and an electromagnetic calorimeter (EMC) in a configuration optimized for the study of high-energy cosmic-ray electrons and positrons. It was launched by high-altitude balloon from Lynn Lake, Manitoba, Canada, at a vertical geomagnetic cutoff rigidity of well below 1 GV, on 23 August 1995, at a time corresponding approximately to a minimum of solar activity. The ascent from an atmospheric overburden at the ground of 960 g/cm^2 to a float altitude at 3 g/cm^2 required 3.1 hours, during which charged atmospheric secondary particles were detected and recorded. In identifying muon events, the TRD is not used. The TOF system measures the velocity of the particle $\beta = v/c$ with a resolution of $\sigma_\beta = 0.15$, permitting complete rejection of upward-going events; in addition, the amount of light deposited in the scintillation counters of the TOF system is used to measure the magnitude of the particle's electric charge Ze with a resolution of $\sigma_Z = 0.11$, permitting the unambiguous identification of singly-charged particles. The magnet spectrometer measures the sign of the particle's charge from the direction of the deflection in a magnetic field of about 1 T, and the rigidity $R = pc/Ze$ of the particle from the amount of deflection; at rigidities between 0.3 and 0.9 GV, the resolution achieved is $\sigma_R = 0.08$ to 0.11 GV. The EMC records the pattern of energy deposits in 10 scintillation counters, each underneath a 0.9 radiation length-thick lead sheet. In each layer, the energy deposited is measured in units of the energy loss by a vertical minimum-ionizing particle (MIP). A shower sum is obtained by adding the signals from the 10 scintillators.

The selection of muon events is described in detail elsewhere (Tarlé et al. 1997). First, a high-quality spectrometer track and measurement of the rigidity R, and downgoing and singly-charged TOF characteristics are required. We select μ^--like events by requiring: 1) $\beta \geq 0.85$ and 2) $R \leq -0.3$ GV. For $R \geq 0.9$ GV, μ^+ events become indistinguishable from non-showering hadrons (mostly protons), so that μ^+ spectra are not measured with this instrument. We also require that particles not shower in the EMC (EMC sum $\leq$ 15 MIPs). With these criteria, we achieve essentially complete rejection of electron events, but there remains a small background to the muon signal due to pions and kaons. We estimate from Monte Carlo simulations of air showers based on CERN's GEANT-FLUKA algorithms (Fassò et al. 1993) that the $\pi^\pm$ flux at a depth of 13 g/cm^2 is only 2% that of $\mu^\pm$, in agreement with another calculation (Stephens 1981) – with $K^\pm$ fluxes at a much lower level – and that this further decreases with increasing atmospheric depth. Moreover, only pions that do not shower can be mistaken for muons, which occurs 39% of the time, so that the background to the muon measurement due to atmospheric pions is only about 0.7-0.9% near float, dropping to less than 0.4% at depths greater than 300 g/cm^2. Such a small background is not corrected for here. Occasionally, cosmic-ray interactions in the instrument result in $\pi^\pm$ production, at an even more modest level than the atmospheric pion background. GEANT-based simulations indicate that only 0.04% of proton-induced events yield a misidentification as a μ^-.

R (GV)	$\overline{R}$ (GV)	ϵ_{dt} (%)	(ΩA) (cm^{2}sr)	ϵ_{acc} (%)
0.3-0.5	0.40	68.35±0.22	568.9±2.6	52.0±0.5
0.5-0.8	0.65	74.46±0.20	613.1±2.8	63.0±0.5
0.8-1.2	0.99	78.77±0.19	608.2±2.7	66.1±0.5
1.2-1.7	1.43	80.46±0.18	604.4±2.7	65.4±0.5
1.7-2.5	2.06	81.57±0.18	600.0±2.7	64.6±0.5
2.5-4	3.13	81.64±0.18	601.9±2.7	63.9±0.5
4-8	5.52	81.48±0.18	598.9±2.7	62.5±0.5
8-16	11.0	81.45±0.18	603.6±2.7	61.2±0.5
16-32	21.3	81.45±0.18	606.0±2.7	47.0±0.4
32-50	39.2	81.43±0.18	602.4±2.7	15.5±0.2

Table 1: Rigidity-dependent parameters and corrections used in the determination of the absolute μ^- intensities.

3 Results and Discussion

The absolute intensity of μ^-, at a rigidity $\overline{R}$ within ΔR, at atmospheric depth d is obtained with:

$$j_\mu(d,\overline{R}) = \frac{N_\mu}{\Delta t \epsilon_t \epsilon_l \epsilon_{ps} \epsilon_\theta \epsilon_{dt} \Delta R (\Omega A) \epsilon_{scan} \epsilon_{acc}},$$

where N_μ is the number of μ^- events recorded at (d, R), Δt is the time spent at depth d, ϵ_t is the live time fraction, ϵ_l is an event-transmission loss correction, ϵ_{ps} is a correction to account for a trigger prescaling enabled near the end of ascent to preferentially accept events with a shower in the EMC, ϵ_θ is a correction to account for the fact that the muon flux is increasingly less isotropic deeper in the atmosphere, ϵ_{dt} is the efficiency of the basic event cleanliness criteria applied to the drift-tube hodoscope track, (ΩA) is the geometrical factor, ϵ_{scan} is a "scanning efficiency" correction (described below), and ϵ_{acc} is the muon acceptance efficiency.

Both $\overline{R}$ and ΔR are weighted to account for the details of the energy spectrum, according to:

$$\overline{R} = \frac{\int_{R_i}^{R_j} R f(R) dR}{\int_{R_i}^{R_j} f(R) dR} \qquad \Delta R = \frac{\int_{R_i}^{R_j} f(R) dR}{f(\overline{R})}$$

where $f(R) \propto R^{-\alpha}$ is the rigidity power-law spectrum, with spectral index α varying between -0.56 and 3.5 depending on both R and d (α is experimentally determined from the spectra before any of the normalization corrections are applied). Δt is measured with an on-board clock, ϵ_t is determined using on-board scalers which count clock cycles while the instrument is available for a trigger or busy processing an event, and ϵ_l is determined by careful accounting of event numbers generated on board compared to events successfully transmitted. ϵ_{ps} is determined by a study of trigger rates before and after the prescaler is enabled, and is found to be $\epsilon_{ps} = (16.2 \pm 0.2)\%$ at 3-13 g/cm^2, 86.3% at 13-32 g/cm^2, and 100% at other depths. ϵ_θ is calculated using a standard prescription (Blokh et al. 1977). ϵ_{dt} is obtained by a careful accounting of the number of events recorded compared to the number of events with a succesful minimal track reconstruction. (ΩA) and ϵ_{acc} are determined with the aid of a GEANT-based simulation of the response of the HEAT instrument. ϵ_{scan} is a correction factor introduced based on the visual scanning of several hundred events to account for residual differences between the reconstruction efficiency of

d (g/cm^2)	$\overline{d}$ (g/cm^2)	Δt ($\pm$1 s)	ϵ_t (%)	ϵ_l (%)	ϵ_θ (%)
3-4	3.45	4203	85.4$\pm$1.3	86.254$\pm$0.078	99.95
4-7	5.13	1509	85.7$\pm$1.4	85.59$\pm$0.13	99.93
7-13	9.85	1199	86.6$\pm$1.1	85.25$\pm$0.15	99.87
13-32	23.2	1453	48.1$\pm$1.8	89.190$\pm$0.079	99.68
32-67	49.1	1307	41.9$\pm$1.6	96.585$\pm$0.047	99.33
67-140	105	1571	49.5$\pm$4.6	95.051$\pm$0.051	98.58
140-250	190	1285	65.8$\pm$6.9	92.894$\pm$0.072	97.45
250-350	298	484	82.9$\pm$0.3	95.45$\pm$0.12	96.05
350-840	499	1163	95.7$\pm$0.2	94.30$\pm$0.14	93.50
840-960	957	5335	99.3$\pm$0.1	97.09$\pm$0.10	88.03

Table 2: Depth-dependent parameters and corrections used in the determination of the absolute μ^- intensities.

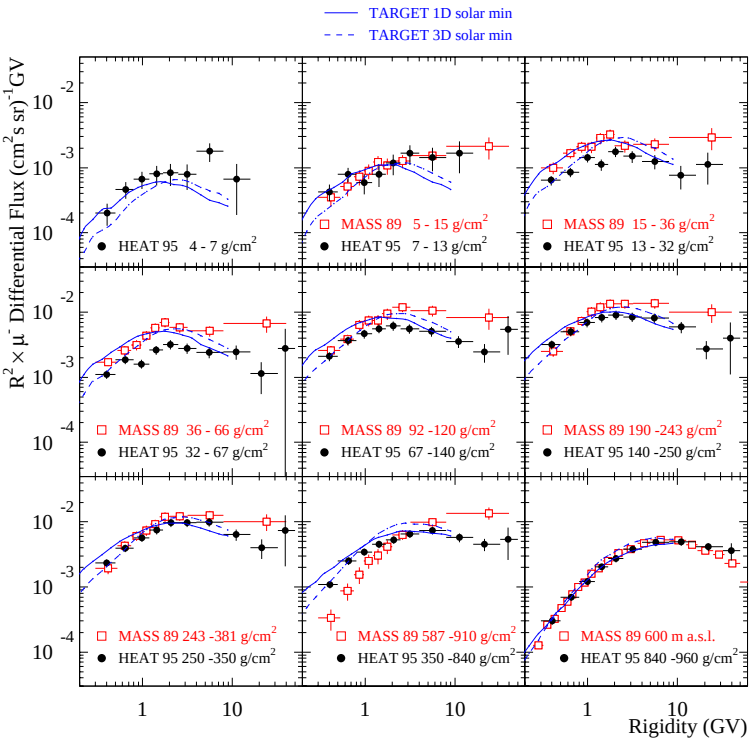

Figure 1: Differential μ^- rigidity spectra as a function of atmospheric depth. The curves are preliminary calculations with the TARGET algorithm.

real events compared to that of simulated ones, and is found to be $\epsilon_{scan} = (0.9 \pm 0.1)$. The various parameters described above are given in Tables 1 and 2.

The final μ^- intensities as a function of rigidity and atmospheric depth are shown in Figure 1. A complete table of all intensities is available on the Web (HEAT muon intensities 1999). Also shown in the figure are the measurements of the MASS experiment (Bellotti et al. 1996). The HEAT sample of 10665 μ^- events at 3-840 g/cm^2 represents a factor of 3.7 improvement over the MASS sample of 2893 events. Although the MASS measurements were also made at Lynn Lake, the flight occurred at a different solar epoch (1989), at the time of a significant Forbush decrease, and, moreover, different atmospheric bin depths were used. The HEAT and MASS data are therefore not directly comparable, but the general level of agreement between the two data sets is encouraging. Finally, we also show in Figure 1 preliminary calculations with the TARGET algorithm (Agrawal et al. 1996, Stanev & Gaisser 1998) at solar minimum. In addition to calculations obtained with the traditional one-dimensional air shower development code (solid curves), calculations are presented with a new version of the software where shower development is performed in three dimensions (dashed curves). Geomagnetic effects are not included in the calculations. It is not possible within the statistical errors to differentiate between the two calculations. The simulated distributions appear to be substantially in agreement with the measurements at atmospheric depths greater than about 140 g/cm^2, where the bulk of atmospheric muons and neutrinos are produced. At shallower depths, small differences between the measurements and the model predictions exist, which would not significantly affect the flux of atmospheric neutrinos.

Acknowledgements

We are grateful to T. Stanev and T. K. Gaisser for helpful discussions, and for sharing with us their TARGET Monte Carlo algorithm. We thank the NSBF balloon crews that have supported the HEAT flights. This work was supported by NASA grants NAG5-5059, NAG5-5069, NAG5-5070, NAGW-5058, NAGW-1995, NAGW-2000 and NAGW-4737, and by financial assistance from our universities.

References

Aglietta, M. et al. 1989, Europhys. Lett. 8, 611
Agrawal, V. et al. 1996, Phys. Rev. D 53, 1314
Barbiellini, G. et al. 1997, Proc. of the 25th ICRC (Durban) 6, 317
Barr, G. et al. 1989, Phys. Rev. D 39, 3532
Barwick, S. W. et al. 1997, Nucl. Instr. Meth. A 400, 34
Becker-Szendy, R. et al. 1992, Phys. Rev. D 46, 3720
Bellotti, R. et al. 1996, Phys. Rev. D 53, 35
Berger, C. et al. 1989, Phys. Lett. B 227, 489
Blokh, Y. L. et al. 1977, Nuov. Cim. B 37, 198
Fassò, A. et al. 1993, Proc. of the IVth Int. Conf. on Calorimetry in High Energy Physics (La Biodola)
Fukuda, Y. et al. 1994, Phys. Lett. B 335, 237
Fukuda, Y. et al. 1999, Phys. Rev. Lett. 82, 2644
Goodman, M. et al. 1995, Nucl. Phys. B (Proc. Suppl.) 38, 337
HEAT muon intensities 1999, http://pooh.physics.lsa.umich.edu/www/heat/mufluxes.html
Honda, M. et al. 1990, Phys. Lett. B 248, 193
Kawasaki, M., & Mizuta, S. 1991, Phys. Rev. D 43, 2900
Krizmanic, J. F. et al. 1997, Proc. of the 24th ICRC (Rome) 1, 593
Lee, H., & Koh, Y. S. 1990, Nuov. Cim. B 105, 883
Schneider, E. et al. 1995, Proc. of the 24th ICRC (Rome) 1, 690
Stanev, T., & Gaisser, T. K. 1998, private communication
Stephens, S. A. 1981, Proc. of the 17th ICRC (Paris) 4, 282
Tarlé, G. et al. 1997, Proc. of the 25th ICRC (Durban) 6, 321